Plasma Sci. Technol. **25** (2023) 125001 (10pp) https://doi.org/10.1088/2058-6272/ace1d4

Study of a collisionless magnetized plasma sheath with nonextensively distributed species

R PAUL[1], K DEKA[1], G SHARMA[1], R MOULICK[1], S ADHIKARI[2], S S KAUSIK[1,*] and B K SAIKIA[1]

[1] Centre of Plasma Physics, Institute for Plasma Research, Assam 782402, India
[2] Institute for Energy Technology, Instituttveien 8, Kjeller 2007, Norway

E-mail: kausikss@rediffmail.com

Received 27 March 2023, revised 26 June 2023
Accepted for publication 26 June 2023
Published 28 August 2023

Abstract

A weakly magnetized sheath for a collisionless, electronegative plasma comprising positive ions, electrons, and negative ions is investigated numerically using the fluid approach. The electrons are considered to be non-Maxwellian in nature and are described by Tsalli's distribution. Such electrons have a substantial effect on the sheath properties. The study also reveals that non-Maxwellian distribution is the most realistic description for negative ions in the presence of an oblique magnetic field. In addition to the negative ion temperature, the sheath potential is also affected by the nonextensive parameters. The present research finds application in the plasma processing and semiconductor industry as well as in space plasmas.

Keywords: magnetised plasma sheath, electronegative plasma, non-extensive distribution

(Some figures may appear in colour only in the online journal)

1. Introduction

The intricacies of sheaths have made them one of the most researched topics in plasma physics. Although they have been studied and understood by both fluid [1–7] and kinetic approaches [8–12], there is enough scope to investigate the problem further. In the case of the fluid approach, usually, the ions are governed by the hydrodynamic equations and the distribution of electrons are defined by Maxwell–Boltzmann statistics. However, it is often realized that although the Maxwellian approach is simplistic, it overlooks several details [13]. Besides, the electrons found in astrophysical plasmas [14, 15] possess a high energy tail and hence the distribution deviates from the Maxwellian nature. It is also proven that the electrons found in the processing chambers are also far from being Maxwellian [16, 17]. Generally, laboratory plasmas are found to have a high energy tail, thus losing their Maxwellian identity [18, 19]. Moreover, the Boltzmann behaviour restricts the electron distribution to the macroscopic ergodic equilibrium state and is often found to be inadequate to describe long-range interactions [20]. Also, the plasma sheath is regarded as a transition region between the plasma and the wall and is considered a non-neutral region besides possessing a non-Maxwellian nature [12, 21]. Due to such characteristics, the sheath plays a substantial role in influencing the particle and energy transport towards the wall. Therefore, the hunt persists for a more generalized version of Boltzmann–Gibbs statistics that could provide a better description of such non-Maxwellian behaviour.

In 1988, Tsallis proposed an entropy for systems that are no longer in an ergodic equilibrium state and it is defined as [22]

$$S_q = k_{\mathrm{B}}\left(\frac{1-\sum_i p_i^q}{q-1}\right),$$

where p_i is the probability of the ith microstate, k_{B} is the Boltzmann constant and q is a real number. In this case, q measures the degree of nonextensivity [22–25]. Usually, the entropy for an entire system in equilibrium is the summation of the entropies of their respective parts. However, this is not

* Author to whom any correspondence should be addressed.

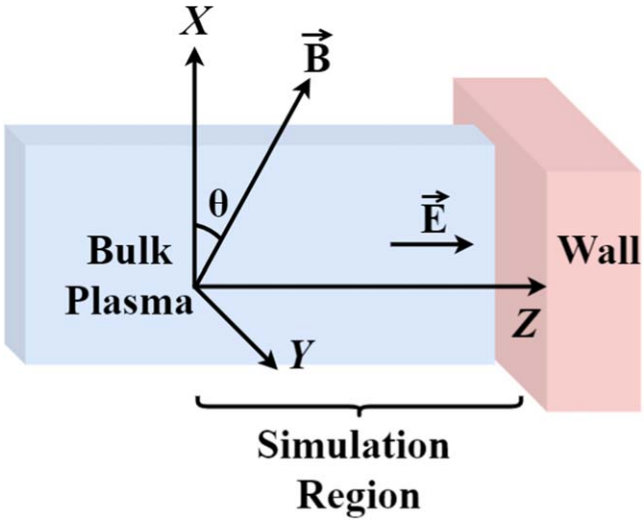

Figure 1. Geometry of the system.

the case for a nonextensive system. In such systems, the generalized entropy of the system is either greater than the sum of its parts for $q > 1$ or smaller than the sum when $q < 1$. Boltzmann–Gibbs entropy can be derived from q-entropy [20, 25]. This distribution is found to be more suitable for those systems where long-range particle interactions are more prevalent. To describe the nonextensive nature of the plasma, it is introduced in the system via electrons. Huibin Qiu *et al* [26] have measured the electron nonextensive parameter using a nonextensive single electric probe and found it to be 0.775.

Furthermore, the nonextensive distribution studies have provided meaningful insights while investigating complex problems such as ion-acoustic waves [27], dust charging [28] or in understanding solitary structures [29]. In addition, the behaviour of nonextensive electrons on the sheath structures has also been widely studied. Gougam and Tribeche [30] studied the Debye shielding phenomenon considering both nonextensive electrons and ions. They found that the debye length in the case of nonextensive electrons is smaller compared to the standard Maxwellian case. Besides investigating the role of the nonextensive parameter, Moulick *et al* [31] studied the effect of ion-neutral collision in the presheath and sheath region. Moreover, multi-electron species described by nonextensive distribution have been studied by Borgohain *et al* [32] using the Sagdeev pseudo-potential method and they concluded that the ion entrance velocity depends upon the temperature of the ions, the temperature and the density ratio of the electron species.

In addition to multi-electron plasma, the sheath, along with additional components such as negative ions, in the presence of, as well as in the absence of, magnetic field has been studied considering nonextensive electrons [33, 34]. In all such investigations, negative ions are considered to be Maxwellian in nature. It emerges as an apt choice with the justification that the magnetic field has a negligible effect on the negative ions as compared to the positive ions [35]. This provides the balance between the electric field force and the pressure force, therefore, retaining the Boltzmannian behaviour. As the inertia of the negative ions is larger than that of the electrons, this acts as the point of contention for choosing Maxwellian distribution. Also, considering Maxwellian negative ions has resulted in oscillatory structures while studying sheath properties [36, 37]. Such oscillations are not realized if realistic distributions are considered [38]. It is a hint at the possibility that the negative ions might have a non-Maxwellian distribution. Additionally, the negative ion energy is also experimentally found to deviate from the usual Maxwellian nature [39]. Besides, there are instances of considering non-Maxwellian negative ions in understanding the dust charging process [40]. It is quite well known that the negative ions have a notable effect on the sheath structure. Apart from that, the negative ions also find their presence in many industrial applications as well as in fusion devices [41–45]. It is usually favoured over positive ions in the case of neutral beam injection (NBI) as negative ions have greater efficiency in heating the fusion plasma to sustain the desired temperature [46]. Thus, negative ion-rich plasmas provide a promising platform for basic as well as application-related studies.

The present paper aims to understand the nature of negative ions in the presence of an oblique magnetic field and nonextensive electrons. Initially, Maxwellian distributed negative ions are considered and the sheath properties are investigated. Later on, negative ions are considered to be nonextensively distributed. It is seen that the dynamics of positive ions change with the nature of the negative ion distribution. It concludes that the negative ions are better described by a non-Maxwellian distribution under the influence of the magnetic field.

The paper has been divided into the following sections. Section 2 discusses the theoretical model and the basic equations. Section 3 analyzes the theoretical findings and a brief conclusion has been presented in section 4.

2. Theoretical model and basic equations

The present study considers a steady-state multi-component hydrogen plasma comprising hydrogen positive ions, electrons and hydrogen negative ions. The plasma is collisionless and is considered to be in contact with a planar wall. An oblique magnetic field **B**, as shown in figure 1, is considered in the X-Z plane with an angle of inclination, θ, with the X-axis perpendicular to the wall. The sheath is formed along the positive Z-direction. The cold ions are described by the hydrodynamic equations in a 1D-3V representation given by

$$m_i n_i (\mathbf{v} \cdot \nabla)\mathbf{v} = n_i e\mathbf{E} + n_i e(\mathbf{v} \times \mathbf{B}) - m_i S_i \mathbf{v}, \qquad (1)$$

where **B** is the magnetic field intensity, and m_i, **v** are the mass and velocity of the positive ions, respectively.

The first term in the momentum equation (1) represents the electrostatic force, the second term corresponds to the magnetic force and the third term refers to the momentum transfer due to ionization. The ions are usually cold and hence the pressure gradient term may be neglected. However, a finite isotropic ion temperature is considered for the present

case. The magnitude of the ion temperature is small enough to avoid the pressure gradient term. Though, in a magnetized plasma, anisotropy in ion temperature is often encountered which results in numerous instabilities in the plasma [5]. But, the plasma considered in this paper is stable and is devoid of any such anisotropy. On the other hand, the ion-neutral collisions are neglected and the dominant force in the sheath formation is the Lorentz force. Additionally, the momentum transfer due to ionization is neglected in the present case. However, the momentum transfer due to ionization in the momentum equation of the ions is usually responsible for any increase in the ion velocity. But, as compared to the other terms such as the electric force and magnetic force, the transfer of momentum due to ionization is nominal. Thus, any increase in the ion temperature due to ionization will be insignificant and hence ion-neutral collisions can be neglected [47].

The continuity equation is given by

$$\nabla \cdot (n_i \mathbf{v}) = S_i, \tag{2}$$

In this case, an exponential ion source, S_i is considered and can be defined as

$$S_i = n_e \mathbb{Z},$$

where $\mathbb{Z}$ is the ionization rate which is assumed to be constant throughout the domain. S_i represents the rate at which the ions are created per unit volume per unit time [48].

The electrons, being more mobile in nature as compared to the other species, are often represented by the Boltzmann relation, defined as,

$$n_e = n_{e0} \exp \frac{e\phi}{k_B T_e}, \tag{3}$$

where T_e and n_{e0} represent the temperature and equilibrium density of the electrons and ϕ is the electric potential. In such a case, the pressure gradient balances the electric field force [2]. As mentioned above, electron distributions are often found to deviate from Maxwellian nature. It has been found that the Tsallis distribution is best suited for such scenarios. As the present plasma deals with non-Maxwellian electrons, the distribution of the electrons can be defined as

$$n_e = n_{e0}\left[1 + (q-1)\left(\frac{e\phi}{k_B T_e}\right)\right]^{\frac{q+1}{2(q-1)}}, \quad (q < 1) \tag{4}$$

where q is the nonextensive parameter. For $q = 1$, the above equation behaves similarly to that of the Boltzmann relation. The nonextensive parameter q has been largely distinguished into two sections, namely superextensive and subextensive. Superextensive ($q < 1$) corresponds to cases where most of the particles are considered to be fast-moving and possess a high-energy tail. The subextensive cases ($q > 1$) contain low energetic particles mostly [49]. However, the present study focuses mostly on the presence of high energetic particles and the superextensive case is best suited for such a model.

In the case of negative ions, they have been defined by the Boltzmann relation as

$$n_- = n_{-0} \exp \frac{e\phi}{k_B T_-}, \tag{5}$$

where T_- and n_{-0} represent the temperature and equilibrium density of the negative ions. The reason behind the Boltzmann behaviour for negative ions is that the magnetic field has a negligible effect on them as compared to the positive ions [35]. Also, the negative ions are pushed by the electric field towards the centre of the discharge, thereby a decrease in the velocities is observed which aids in balancing the electric field force with the pressure gradient. This validates the reason for choosing the Boltzmann relation [5].

Asserghine *et al* [34] and Zou *et al* [50] have studied the effect of the nonextensive electrons on the electronegative plasma sheath in the presence of an oblique magnetic field. However, as the focus of both the studies lies on the Debye sheath, they have equated the sheath edge velocities to the Mach number. This also, in turn, implies that the presheath region is not considered in their study. On the other hand, in the present study, the presheath region is considered and thus the equations are scaled in the ionization length scale. Considering the 1D-3V representation of the system, the equations can be resolved into components along the *X, Y* and *Z* directions as

$$v_Z \frac{dv_X}{dZ} = \omega_Z v_Y - \frac{n_e \mathbb{Z}}{n_i} v_X, \tag{6}$$

$$v_Z \frac{dv_Y}{dZ} = (\omega_X v_Z - \omega_Z v_X) - \frac{n_e \mathbb{Z}}{n_i} v_Y, \tag{7}$$

$$v_Z \frac{dv_Z}{dZ} = -em_i \frac{d\phi}{dZ} - \omega_X v_Y - \frac{n_e \mathbb{Z}}{n_i} v_Z, \tag{8}$$

$$\frac{d(n_i v_Z)}{dZ} = n_e \mathbb{Z}. \tag{9}$$

The electrostatic potential is governed by Poisson's equation

$$\frac{d^2\phi}{dZ^2} = -\frac{e}{\epsilon_0}(n_i - n_e - n_-). \tag{10}$$

To solve the above set of equations, it is necessary to normalize the quantities by the following dimensionless parameters

$$u = \frac{v_X}{c_s}, \quad v = \frac{v_Y}{c_s}, \quad w = \frac{v_Z}{c_s},$$

$$\gamma_X = \frac{\omega_X \lambda_{ni}}{c_s}, \quad \gamma_Z = \frac{\omega_Z \lambda_{ni}}{c_s}, \quad \beta = \frac{\mathbb{Z}\lambda_{ni}}{c_s},$$

$$\xi = \frac{Z}{\lambda_{ni}}, \quad \eta = -\frac{e\phi}{kT_e}, \quad \lambda_{ni} = \frac{c_s}{\mathbb{Z}},$$

$$N_i = \frac{n_i}{n_{i0}}, \quad N_e = \frac{n_e}{n_{i0}}, \quad N_- = \frac{n_-}{n_{i0}},$$

$$\alpha = \frac{n_{-0}}{n_{e0}}, \quad \delta = \frac{n_{e0}}{n_{i0}}, \quad 1 - \delta = \frac{n_{-0}}{n_{i0}}$$

$$\delta = \frac{1}{(1+\alpha)}$$

Table 1. List of simulation parameters.

Electron temperature, T_e	1 eV
Ion temperature, T_i	0.026 eV
Positive ion mass, m_i	1 AMU
Ionization frequency, $\mathbb{Z}$	1×10^5 s^{-1}
Bulk plasma density, n_0	5×10^{18} m^{-3}
Magnetic field intensity (External), B_0	1.0 T
Magnetic field inclination, θ	15°

$$\tau_i = \frac{T_i}{T_e}, \quad \tau_- = \frac{T_e}{T_-}.$$

where,

$$c_s = \sqrt{\frac{kT_e}{m_i}}, \quad \lambda_D = \sqrt{\frac{\epsilon kT_i}{n_{e0}e^2}}$$

$$\omega_X = \frac{eB_X}{m_i} = \frac{eB_0\cos\theta}{m_i}$$

$$\omega_Z = \frac{eB_Z}{m_i} = \frac{eB_0\sin\theta}{m_i}$$

ω_X and ω_Z are the respective ion-cyclotron frequencies along the X and Z directions.

The normalized equations are given by

$$\frac{du}{d\xi} = \gamma_Z\left(\frac{v}{w}\right) - \beta\frac{N_e}{N_i}\frac{u}{w}, \tag{11}$$

$$\frac{dv}{d\xi} = \gamma_X - \gamma_Z\left(\frac{u}{w}\right) - \beta\frac{N_e}{N_i}\frac{v}{w}, \tag{12}$$

$$\frac{dw}{d\xi} = \frac{1}{w}\frac{d\eta}{d\xi} - \gamma_X\left(\frac{v}{w}\right) - \beta\frac{N_e}{N_i}, \tag{13}$$

$$\frac{dN_i}{d\xi} = 2\beta\frac{N_e}{w} - \frac{N_i}{w^2}\frac{d\eta}{d\xi} - \gamma_X\left(\frac{N_i}{w^2}\right)v, \tag{14}$$

$$\frac{d^2\eta}{d\xi^2} = \tau_i a_0(N_i - N_e - N_-), \tag{15}$$

where

$$a_0 = \left(\frac{\lambda_{ni}}{\lambda_D}\right)^2.$$

The normalized electron and negative ion densities are given by

$$N_e = \delta[1 - (q-1)\eta]^{\frac{q+1}{2(q-1)}}, \quad N_- = (1-\delta)\exp(-\eta\tau_-). \tag{16}$$

2.1. Numerical techniques

The above set of equations (11)–(15) are ordinary differential equations that can be solved using the Runge-Kutta fourth order method. As these are initial valued problems, the initial values are obtained from the Taylor series expansion [4, 51, 52]. The series may be constructed as

$$V_i = V_{i1}\xi + V_{i2}\xi^3 + \ldots$$

$$\eta = \eta_1\xi^2 + \eta_2\xi^4 + \ldots$$

$$N_i = N_{i0} + N_{i1}\xi^2 + N_{i2}\xi^4 + \ldots$$

where N, V, η represents the density, velocity, and potential, respectively for ions.

The above set of series is used in the governing equations and the first coefficients obtained by the Taylor series are considered the initial values. The first-order coefficients are given as

$$\eta_1 = 0,$$

$$u_1 = \frac{\gamma_X\gamma_Z N_{e0}}{4N_{e0}^2 + \gamma_Z^2},$$

$$v_1 = \frac{2\gamma_X N_{e0}^2}{4N_{e0}^2 + \gamma_Z^2},$$

$$w_1 = \frac{N_{e0}}{N_{i0}},$$

$$N_{i0} = 1.$$

At exactly $\xi = 0$, all the physical quantities such as density, velocity, and potential become zero. Therefore, the starting point has been slightly right-shifted from the origin, i.e. $\xi = 0$ such that all the quantities have nonzero physical values.

The default parameters chosen for simulation are in accordance with low-pressure plasma discharges and are listed in table 1.

For the considered plasma parameters, the ion-neutral collisional mean free path ($\lambda_{ni} = 0.33$ m), electron-ion collisional mean free path ($\lambda_{ei} = 0.14$ m), and ion-electron collisional mean free path ($\lambda_{ie} = 29$ m) are large as compared to the length scale of the sheath ($\xi = 9 \times 10^{-4}$ m). Such collisions do not participate in the sheath formation and are, therefore, neglected in the present model. The wall is considered to be floating and is assumed to be situated where the ion flux balances the random electron flux [4, 51, 52]. It is given as

$$n_i v_Z = \frac{1}{4}n_e\bar{c}, \tag{17}$$

where $\bar{c} = \sqrt{\frac{8T_e}{\pi m_e}}$, which is the random velocity of the electron at the wall. In the normalized term, this point is termed as ξ_{wall}. Here, however, the contribution of the negative ion flux is neglected considering the fact that the negative ions are pushed away from the wall by the sheath electric field. This consequently reduces the total incoming flux of negative ions towards the wall and the thermal energy of negative ions is much less than that of the electrons hence its contribution to determining the floating wall condition may be neglected. Additionally, Moulick *et al* [53] have analysed the flux contribution of the total negative species (electrons and negative ions). They found that the negative ion density falls to zero much earlier in space as compared to the electron density. Also, the magnitude of the flux is a very small quantity as compared to the density of the negative ions. Moreover, a similar observation can be seen in the present study as well. Here, the negative ion flux ($F_n = \frac{1}{4}n_n\sqrt{\frac{8T_n}{\pi m_n}} = 0.0045$) is found to be quite small as compared

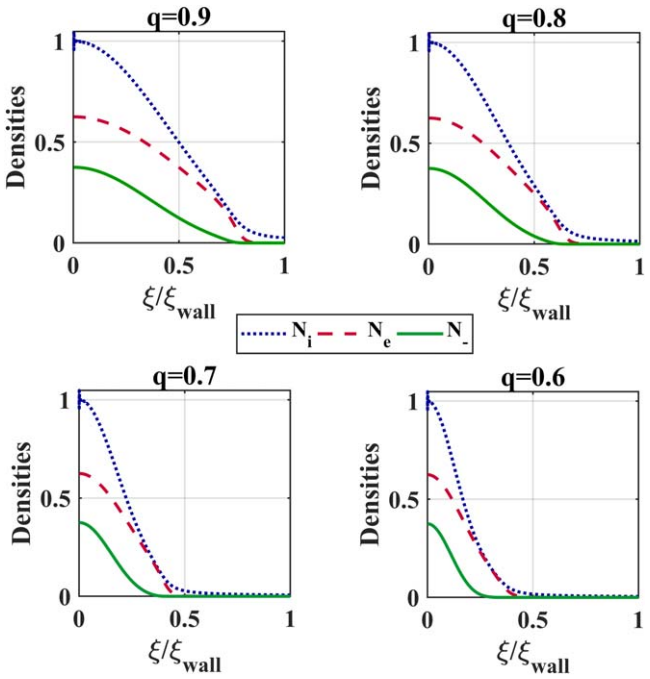

Figure 2. Normalized density of all species for different nonextensive parameters, q and a constant value of $\tau_- = 2$.

to the electron flux ($F_e = \frac{1}{4} n_e \sqrt{\frac{8T_e}{\pi m_e}} = 1.8$) towards the end of the simulation domain. Hence, the overall contribution of the negative ion flux in determining the wall position can be neglected.

3. Results and discussions

3.1. Negative ions described by Boltzmann distribution

To understand the effect of nonextensive electrons on various sheath parameters, an investigation into spatial variation of the density of the species can provide meaningful insight into the problem. Figure 2 shows the normalized density variation with respect to the different q parameters for an electron-rich plasma ($\alpha < 1$) and for that reason α is chosen to be 0.6 [5]. For the present case, $\tau_- = 2$ such that the negative ion temperature lies within the well-established limits [54], and also to avoid any multi-valued plasma potential solution [55]. The variation in the q parameter greatly affects the density descent of all the species along the sheath. With the decrease in the q value, the density of the individual species declines rapidly as can be seen in figure 2. The distribution corresponding to lower q values is wider. As a result, such distributions have more high energetic electrons as compared to higher q values. This consequently compels the positive ions to complete the shielding process faster, thereby leading to a quick fall. The negative ions, on the other hand, follow the positive ions and limit themselves near the core region. The density fall becomes rapid for lower q value, which has been earlier observed by Borgohain *et al*, for an electrostatic case [33]. Particularly in the case of the positive ions, they are

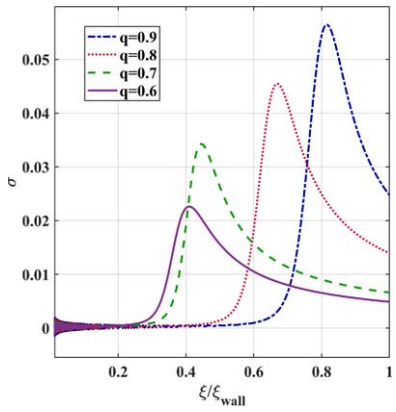

Figure 3. Normalized space charge profile for different nonextensive parameters, q and for constant values of $\alpha = 0.6$ and $\tau_- = 2$.

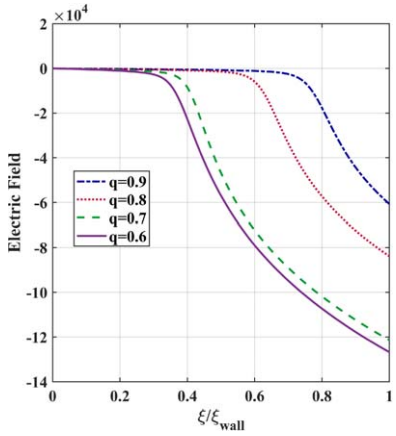

Figure 4. Normalized electric field profile for different nonextensive parameters, q and a constant values of $\alpha = 0.6$ and $\tau_- = 2$.

unable to complete the gyration due to the drift experienced by the guiding centre as a consequence of the rapid motion of the species [47]. This implies that the magnetic field has a moderate effect on the ions.

The nonextensive electrons have an effect on another important sheath parameter, namely the space charge profile, which can be seen in figure 3. The space charge profile is often considered a way to visualize the sheath thickness in plasma. The charge deposition in this case decreases near the wall with the decrease in the q parameter, as well as the peak shifts towards the sheath edge. This can be justified as the rapid fall of the negative species with a lower q value occurs near the edge region. This results in the screening of the negative species by the ions at the entrance edge which creates a non-neutral region far away from the wall. The electric field profile depicted in figure 4 also confirms that the net positive charge distribution inside the sheath increases with the decrease in the q parameter. For $q = 0.9$, the charge separation is localized near the wall and this lowers the electric field. With the gradual decrease in the q value, this localized nature gradually disappears and the overall broadening of the positive space charge region occurs which is visible from figure 3. Additionally, the ion entrance velocity

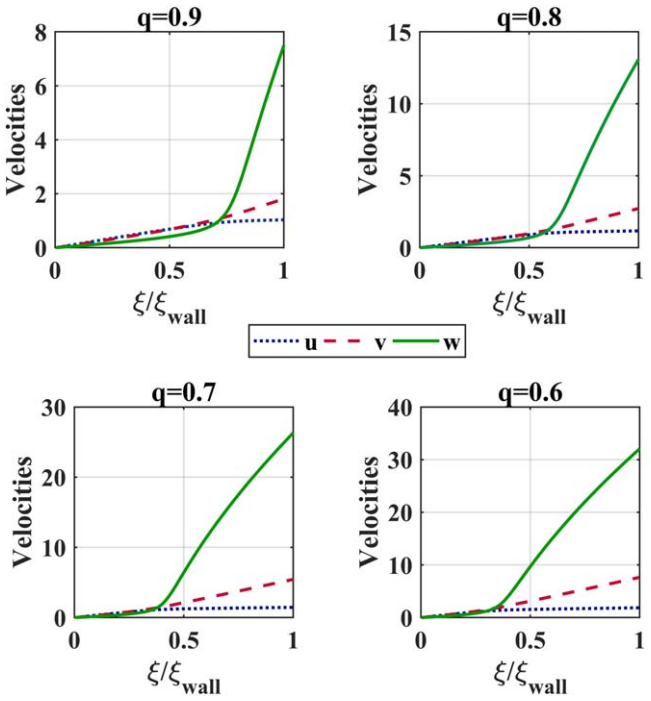

Figure 5. Normalized velocities along the X , Y and Z directions for different nonextensive parameters, q and for constant values of $\alpha = 0.6$ and $\tau_{-} = 2$.

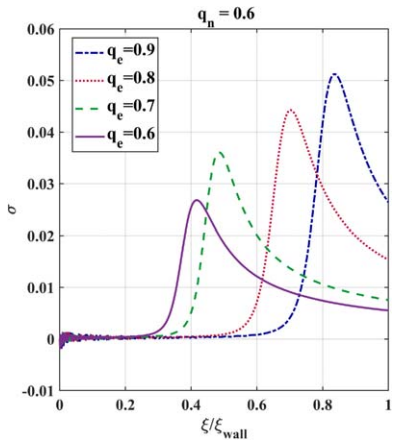

Figure 6. Normalized space charge profile for different electron nonextensive parameters, q_{e} and for constant values of negative-ion nonextensive parameter, q_{n}, $\alpha = 0.6$ and $\tau_{-} = 2$.

along the Z component also decreases with the lower q value, which can be observed in figure 5. This affects the space charge amplitude and is, therefore, found to be least for $q = 0.6$, as observed in figure 3. However, the velocity increases monotonically for lower q values.

3.2. Negative ions described by q nonextensive distribution

Now, considering a more realistic situation where negative ions can also deviate from the usual Maxwellian nature, here a nonextensive distribution is used to describe them. It is defined as

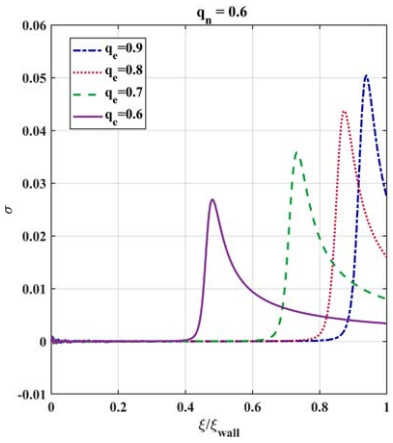

Figure 7. Normalized space charge profile for different electron nonextensive parameters, q_{e}, and for constant values of negative-ion nonextensive parameter, q_{n}, $\alpha = 0.6$ and $\tau_{-} = 2$ for a bulk density of 10^{20} m^{-3}.

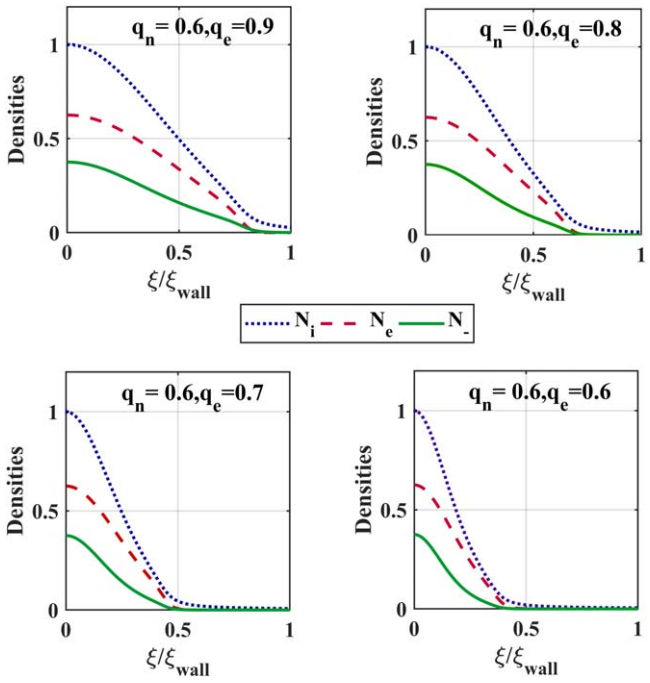

Figure 8. Normalized density of all species for different nonextensive parameters, q_{e}, and for constant values of q_{n}, $\alpha = 0.6$ and $\tau_{-} = 2$.

$$n_{-} = n_{-0}\left[1 + (q-1)\left(\frac{e\phi}{kT_{-}}\right)\right]^{\frac{q+1}{2(q-1)}}, \qquad (q < 1) \tag{18}$$

The normalized density is given by

$$N_{-} = (1-\delta)[1 - (q-1)\eta\tau_{-}]^{\frac{q+1}{2(q-1)}}. \tag{19}$$

However, the parameter q for negative ions and electrons is chosen to be different. Thus, the normalized density equations (4) and (18) become

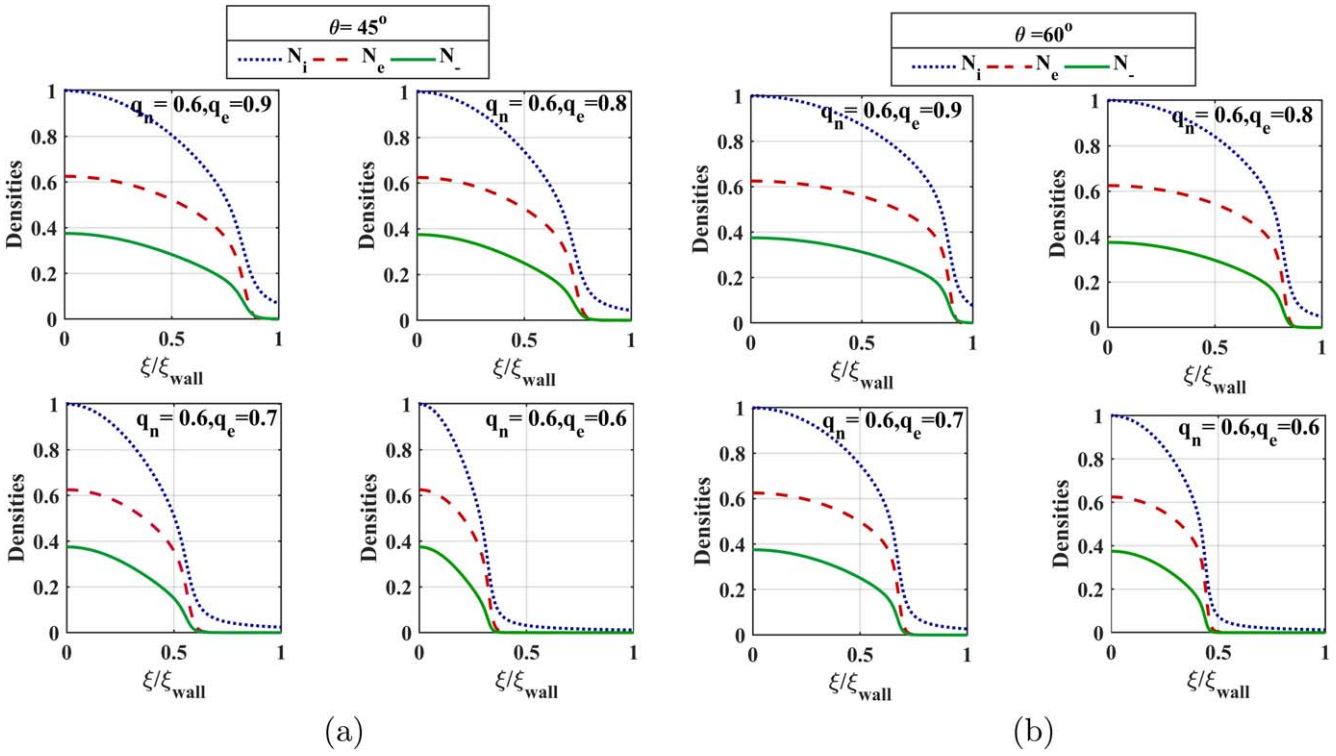

Figure 9. Normalized density of all species for different nonextensive parameters, q_e at different magnetic field inclinations, θ and for constant values of q_n, $\alpha = 0.6$ and $\tau_- = 2$.

$$N_e = \delta[1 - (q_e - 1)\eta]^{\frac{q_e+1}{2(q_e-1)}}, \tag{20}$$

$$N_- = (1 - \delta)[1 - (q_n - 1)\eta\tau_-]^{\frac{q_n+1}{2(q_n-1)}}. \tag{21}$$

where q_e, q_n are the q parameters for electrons and negative ions, respectively.

Here the sheath parameters are investigated in the presence of nonextensive electrons as well as nonextensive negative ions. On the onset, the space-charge profile for different q_e values corresponds to a particular value of q_n, $\alpha = 0.6$ and $\tau_- = 2$ is plotted in figure 6. It is seen that the non-neutral region appears broader in this case, indicating a lower charge separation between the bulk region and the wall. Moreover, the numerical noise has been reduced to a certain extent by choosing non-extensive negative ions. For a high-density plasma ($n_0 = 1 \times 10^{20}$ m^{-3}) the noise further reduces, indicating that the non-Maxwellian nature dominates in such scenarios. Although, the density of the majority charge contributor is low, as seen in figure 7. However, the overall negative charge density has increased inside the sheath. This can be very well observed from the density profile, as seen in figure 8. The negative ions have a slower fall for lower q_e values as compared to the Maxwellian negative ions and the overall particle density has increased inside the sheath.

Also, while choosing the distribution for negative ions, it is always considered that the magnetic field influence is negligible on the negative ions. However, the density distributions in figures 9(a) and (b) show quite an interesting behaviour. The magnetic field inclination is believed to have an impact on the spatial distribution of the species towards the wall. Thus, a consequential consideration of magnetic field inclination becomes essential.

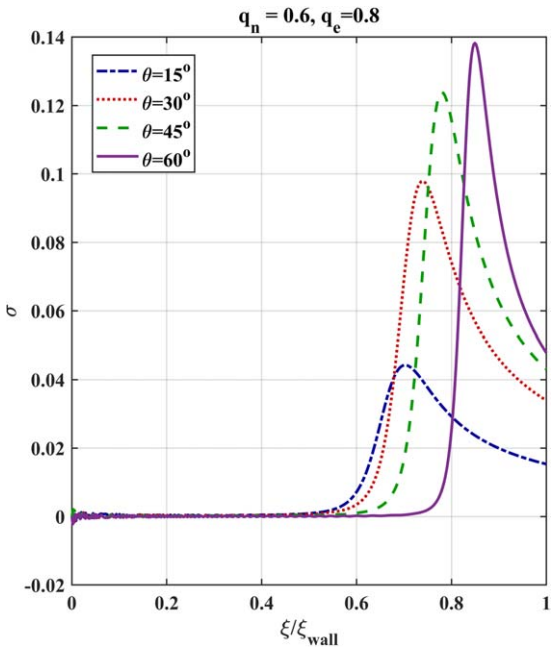

Figure 10. Normalized space charge profile for different magnetic field inclinations, θ.

3.2.1. Effect of magnetic field inclination, θ. As the species are found to have a dependence on the magnetic field, the problem has been further investigated by varying the angle of inclination. Here, both the nonextensive q_e and q_n are kept

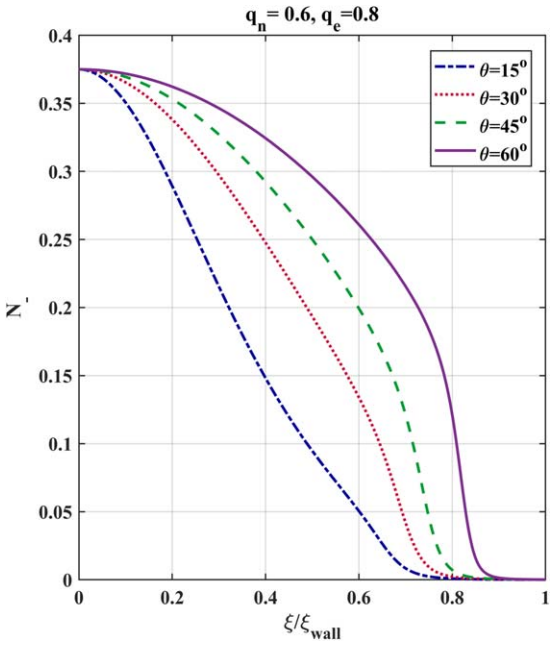

Figure 11. Normalized negative ion density profile for different magnetic field inclinations, θ.

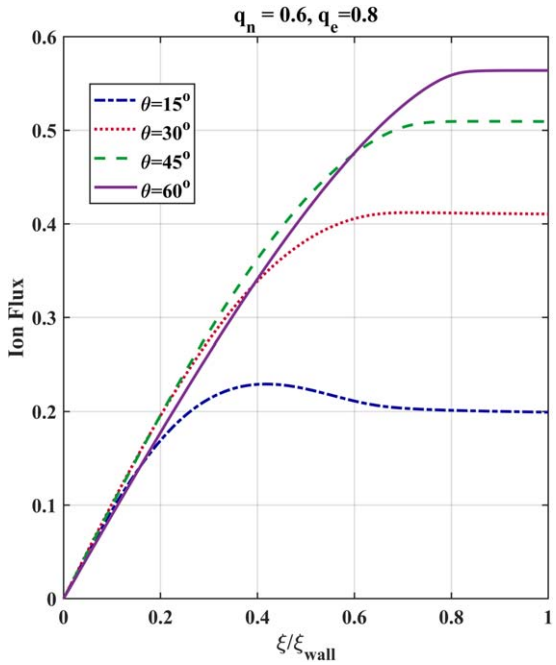

Figure 12. Normalized ion flux profile for different magnetic field inclinations, θ.

fixed. First and foremost, the space charge profile for various magnetic field inclinations has been obtained as shown in figure 10. With the increase in θ, the span of the sheath decreases while the total positive charge deposition increases. The corresponding response of the negative ion distribution across the sheath has been portrayed in figure 11. The nature of the density profile for $\theta = 15^{\circ}$ is found to differ from the other three cases. This behaviour can be purely attributed to the resistive nature of the magnetic force on the motion of the species towards the wall. For increasing θ, the Z-component of the magnetic field decreases, which enables more positive ions to gather near the wall, resulting in higher charge deposition. Consequently, a smaller length is required to shield the sheath electric field. Additionally, due to higher charge deposition, the total ion flux as seen in figure 12 also increases with increasing θ. As negative ions follow the positive ions while traversing towards the wall, this affects the negative ions' motion to a great extent. As a result, it establishes the argument that the role of the magnetic field in the dynamics of the negative ions can not be ignored. Hence, a non-Maxwellian description of the negative ions proves to be the most suitable in such a magnetised scenario.

3.2.2. Discussion on electric potential (η). Another important parameter to investigate the sheath structure is the electric potential profile. It can be well stated that the potential at the wall is sensitive to the change in the value of the q parameter. For a fixed q_n value, figure 13(a) shows the sheath potential variation for different values of q_e and τ_-. It can be observed that as $q_e \to 1$, changes in η are less prominent. However, as q_e becomes more nonextensive, visible changes in η are observed with the change in τ_- values. Additionally, it is observed that η increases as τ_- decreases. For lower values of q_e, the higher energetic tail in the electron distribution function is quite prevalent which increases the mobility of the electrons towards the wall, which in turn increases the net electric field in the sheath. Nevertheless, as $q_e \to 1$, the high energetic tail of the distribution function disappears, thereby lowering the sheath electric field and hence lower values of potential are recorded. Furthermore, for a fixed q_e value, the potential variation for different values of q_n and τ_- is shown in figure 13(b). Here, as τ_- decreases, for any q_n values, η is observed to be minimum. Higher τ_- values indicate cold negative ions hence, any change in the q_n value has a negligible effect on it and thus lower values of electric potential are observed. On the contrary, for lower τ_- i.e. the higher temperature of the negative ions, the overall electric potential increases as $q_n \to 1$. As q_n becomes more nonextensive the potential lowers as compared to $q_n \to 1$, which increases the overall particle density inside the sheath.

As the potential is affected by the temperature of the species, therefore, further investigation into the effect of the electronegativity on the sheath electric potential becomes essential. First and foremost, the wall potential is varied for different electronegativity (α) and q_e values at a constant q_n value and is shown in figure 14(a). It can be observed here that as $q_e \to 1$, the change in α has minimum effect on the potential. However, this scenario changes for lower q_e values. Figure 14(b), on the other hand, shows that the wall potential is varied for different electronegativity (α) and q_n values at a constant q_e value. However, similar observations can be made to that of figure 14(a). This shows that the wall potential is more inclined to the changes in the temperature ratio rather than the electronegativity.

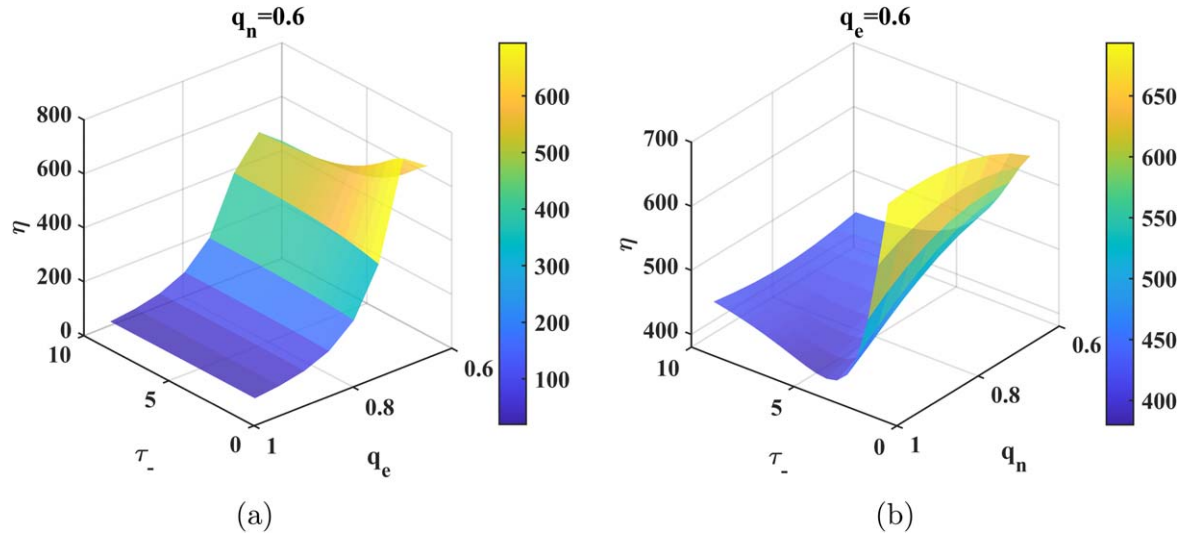

Figure 13. Normalized wall potential variation with temperature ratio (τ_{-}) for (a) constant q_{n} and different q_{e} and (b) constant q_{e} and different q_{n} values for $\alpha = 0.6$.

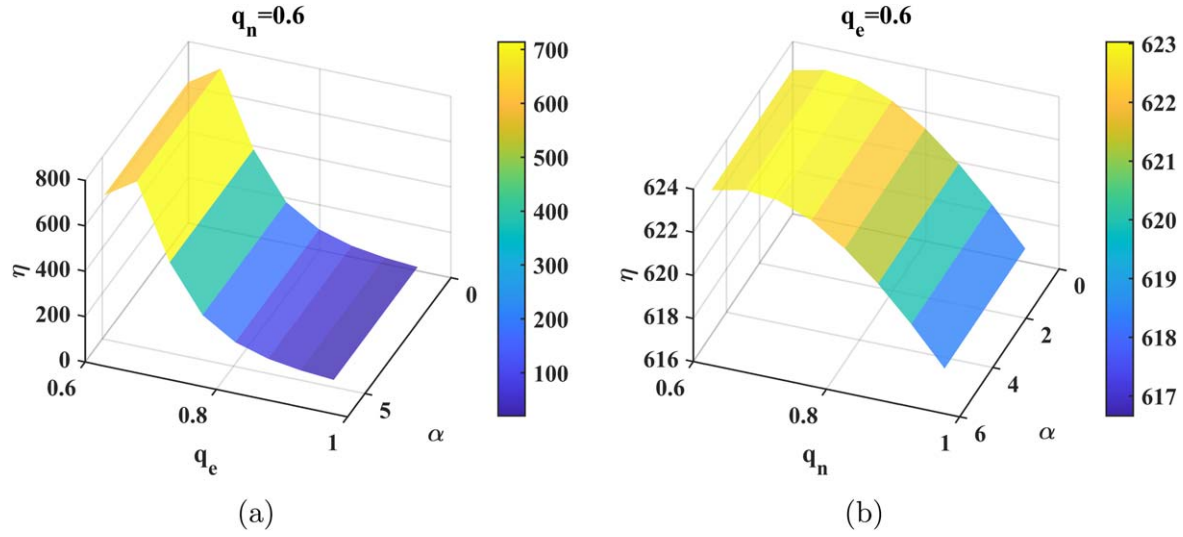

Figure 14. Normalized wall potential variation with electronegativity (α) for (a) constant q_{n} and different q_{e} and (b) constant q_{e} and different q_{n} values for $\tau_{-} = 2$.

4. Conclusion

The present work investigates an electronegative magnetized plasma sheath numerically using the hydrodynamic equations. The electrons are initially considered to be non-extensive while the negative ions are considered to be Boltzmann distributed. As the distribution of electrons shifts away from the Boltzmann, the species tend to fall faster near the core region. This further shifts the charge deposition region away from the wall. It also shows that the magnetic field has a moderate effect on the dynamics of the positive ions. However, in the case of nonextensive negative ions, the scenario changes. The magnetic field inclination plays a major role in the motion of the species. The negative ions also travel a considerable distance inside the sheath. This confirms that the magnetic field influences the negative ions as it affects the positive ions. Also, the numerical noise often observed in the space charge profile is decreased by choosing nonextensive negative ions. Accordingly, it can be concluded that a generalized distribution is a good candidate for describing the negative ions in a multi-component plasma. Additionally, the wall potential is susceptible to changes in the q parameter as well as the temperature of the negative ions. The observations made in the present study might be extended in understanding any plasma surface or material modification fields.

References

[1] Chodura R 1982 *Phys. Fluids* **25** 1628
[2] Beilis I I and Keidar M 1998 *Phys. Plasmas* **5** 1545
[3] Valentini H B and Kaiser D 2014 *Plasma Sources Sci. Technol.* **23** 015004

[4] Moulick R, Adhikari S and Goswami K 2019 *Phys. Plasmas* **26** 043512
[5] Paul R *et al* 2020 *Phys. Plasmas* **27** 063520
[6] Sharma G *et al* 2020 *Phys. Scr.* **95** 035605
[7] Deka K *et al* 2021 *Phys. Scr.* **96** 075606
[8] Bergmann A 1994 *Phys. Plasmas* **1** 3598
[9] Asano K *et al* 2010 *J. Plasma Fusion Res. Ser.* **9** 563 (www.jspf.or.jp/JPFRS/PDF/Vol9/jpfrs2010_09-563.pdf)
[10] Tskhakaya D and Kuhn S 2003 *J. Nucl. Mater.* **313–316** 1119
[11] Adhikari S, Moulick R and Goswami K S 2018 *Phys. Plasmas* **25** 094504
[12] Schiesko L, Wünderlich D and Montellano I M 2020 *J. Appl. Phys.* **127** 033302
[13] Leubner M P 2004 *Phys. Plasmas* **11** 1308
[14] Valentini F 2005 *Phys. Plasmas* **12** 072106
[15] Abid A A *et al* 2017 *Phys. Plasmas* **24** 033702
[16] Hori T *et al* 1996 *Appl. Phys. Lett.* **69** 3683
[17] Safa N N, Ghomi H and Niknam A R 2015 *J. Plasma Physics* **81** 905810303
[18] Kakati B *et al* 2011 *Phys. Plasmas.* **18** 033705
[19] Sharma G *et al* 2022 *Plasma Sources Sci. Technol.* **31** 025013
[20] Hatami M M 2015 *Phys. Plasmas* **22** 013508
[21] Taccogna F *et al* 2007 *J. Nucl. Mater.* **363–365** 437
[22] Tsallis C 1988 *J. Stat. Phys.* **52** 479
[23] Du J 2010 *On the Power-Law q-Distribution Function Based on the Probabilistically Independent Postulate in Nonextensive Statistics* 1
[24] Du J 2004 *Europhys. Lett.* **67** 893
[25] Tsallis C, Mendes R and Plastino A R 1998 *Physica* A **261** 534
[26] Qiu H *et al* 2020 *Phys. Rev.* E **101** 043206
[27] Shalini, Saini N S and Misra A P 2015 *Phys. Plasmas* **22** 092124
[28] Tribeche M and Shukla P K 2011 *Phys. Plasmas* **18** 103702
[29] El Taibany W F and Tribeche M 2012 *Phys. Plasmas* **19** 024507
[30] Gougam L A and Tribeche M 2011 *Phys. Plasmas* **18** 062102
[31] Moulick R, Garg A and Kumar M 2021 *Contrib. Plasma Phys.* **61** e202100047
[32] Borgohain D R, Saharia K and Goswami K S 2016 *Phys. Plasmas* **23** 122113
[33] Borgohain D R and Saharia K 2018 *Phys. Plasmas* **25** 032122
[34] Asserghine A, El Kaouini M and Chatei H 2020 *Materials Today: Proceedings* **24** 24
[35] Aslaninejad M and Yasserian K 2012 *Phys. Plasmas* **19** 033504
[36] Crespo R M *et al* 2012 *Plasma Sources Sci. Technol.* **21** 055026
[37] Yasserian K, Aslaninejad M and Ghoranneviss M 2009 *Phys. Plasmas* **16** 023504
[38] Malik H K and Dhawan R 2020 *IEEE Trans. Plasma Sci.* **48** 2408
[39] Kogut D *et al* 2017 *Plasma Sources Sci. Technol.* **26** 045006
[40] Abid A A *et al* 2016 *Phys. Plasmas* **23** 013706
[41] Stoffels E, Stoffels W W and Kroesen G M W 2001 *Plasma Sources Sci. Technol.* **10** 311
[42] Palop J I F *et al* 1996 *J. Appl. Phys.* **80** 4282
[43] Dubois J P J *et al* 2016 *J. Appl. Phys.* **119** 193301
[44] Ohtake H and Samukawa S 1996 *Appl. Phys. Lett.* **68** 2416
[45] Yasserian K and Aslaninejad M 2010 *Phys. Plasmas* **17** 023501
[46] Kakati B *et al* 2017 *Sci. Rep.* **7** 11078
[47] Adhikari S, Moulick R and Goswami K S 2017 *Phys. Plasmas* **24** 083501
[48] Gyergyek T and Kovačič J 2015 *Phys. Plasmas* **22** 043502
[49] El Ghani O, Driouch I and Chatei H 2020 *Phys. Plasmas* **27** 083701
[50] Zou X *et al* 2020 *Plasma Sci. Technol.* **22** 125001
[51] Forrest J R and Franklin R N 1968 *J. Phys.* D **1** 1357
[52] Valentini H B 2000 *Plasma Sources Sci. Technol.* **9** 574
[53] Moulick R and Goswami K S 2015 *Phys. Plasmas* **22** 033510
[54] Bacal M *et al* 1991 *J. Appl. Phys.* **70** 1212
[55] Allen J E 2009 *Plasma Sources Sci. Technol.* **18** 014004